
One-Shot Transfer Learning for Nonlinear ODEs

Anonymous Author(s)

Affiliation

Address

email

Abstract

1 We introduce a generalizable approach that combines perturbation method and
2 one-shot transfer learning to solve nonlinear ODEs with a single polynomial term,
3 using Physics-Informed Neural Networks (PINNs). Our method transforms non-
4 linear ODEs into linear ODE systems, trains a PINN across varied conditions, and
5 offers a closed-form solution for new instances within the same non-linear ODE
6 class. We demonstrate the effectiveness of this approach on the Duffing equation
7 and suggest its applicability to similarly structured PDEs and ODE systems.

8 1 Introduction

9 Differential equations are crucial in scientific modeling, traditionally solved by methods such as
10 Runge-Kutta and finite element analysis. Recently, Physics-Informed Neural Networks (PINNs)
11 have shown promise in solving ODEs and PDEs by leveraging neural network capabilities (see
12 (6), (8), (10), (15) and reference within). However, computational cost remains a barrier, as PINNs
13 cannot be generalized across different instances of similar equation types (9), (3), a workaround is
14 to train for multiple instances of same equation (4). To address this, we propose a novel hybrid
15 approach that combines the perturbation method with one-shot transfer learning on PINNs (17) to
16 efficiently and accurately solve non-linear ODEs of same type.

17 **Related Work** Introduced in 1998, neural networks for solving differential equations paved the way
18 for today’s Physics-Informed Neural Networks (PINNs) (10), NeuroDiffEq and DeepXDE (13; 2)
19 are two popular software programs that employ PINNs. PINNs have gained popularity and find
20 applications in many domains today, a review of current state-of-the-art applications of PINNs can
21 be found in (6), (11) and (8). PINNs have shown tremendous success in solving complex problems
22 whose analytical solutions don’t exist (1), however they perform poorly with generalizing solu-
23 tions. Work related to adding physical constraints in NN structure (14), bounding errors on PINNs
24 (12), characterizing and mitigating failure modes (9) and improving uncertainty quantification on
25 Bayesian PINNs (5) has been important in increasing reliability of PINNs. PINNs handle interpola-
26 tion problems very well, however face trouble with extrapolation. Transfer learning (TL) methods
27 may be a potential solution, a study of effectiveness of TL can be found in this work (3) and an
28 application can be found here (16). In (16; 18), a multi-headed neural network was used to learn
29 the “latent space” of a class of differential equations. Researchers have developed a transfer learn-
30 ing approach to solve linear differential equations in “one-shot” (17). Extending this to non-linear
31 equations is not possible without modifications since non-linear equations have a non-quadratic loss
32 function which cannot be optimized analytically in one-shot. The head weights have to be learned
33 through an iterative process, such as gradient descent. Our study fills this gap in the literature by
34 extending one-shot transfer learning to non-linear ODEs using perturbation method.

35 2 Methodology

36 We are interested in solving non-linear ODEs with a single polynomial non-linear term of the fol-
37 lowing form:

$$Dx + \epsilon x^q = f(t) \quad (1)$$

38 where D is a differential operator of the form $D = \sum_{j=0}^m g_j \frac{d^j}{dt^j}$ and the RHS is a time-dependent
39 forcing function. Note that we define $g_0 \frac{d^0}{dt^0} x = g_0 x$. The equation is also subject to a boundary
40 conditions: $x(t = 0) = x^*$ and $\frac{d^j}{dt^j} x(t = 0) = x^{(j)*}$ for $j = 1, 2, \dots, m - 1$. Our framework
41 employs perturbation and one-shot transfer learning to solve a specific class of non-linear ODEs.
42 We plan to extend this to handle systems of ODEs and PDEs.

43 Perturbation Method

44 As mentioned above, non-linear ordinary differential equations (ODEs) do not possess analytical
45 solutions to their loss functions with respect to the weights of the linear output layer, which is
46 necessary for one-shot transfer learning.

47 In order to remove the non-linearity in the equation, we approximate the non-linear term ϵx^q as a
48 composition of functions (7). Assume $x = \sum_{i=0}^{\infty} \epsilon^i x_i$, where x_i are unknown functions of t . We
49 approximate x with only p terms as: $x \approx \sum_{i=0}^p \epsilon^i x_i$. It is important to note that this truncated
50 expansion of x is only meaningful when the magnitude of ϵ is less than 1. Furthermore, the p -term
51 approximation is more precise when the magnitude of ϵ is smaller. Fortunately, in most cases, we
52 can adjust the equation by scaling to reduce the magnitude of ϵ . When we substitute the p -term
53 approximation into 1 and expand using multinomial theorem, we obtain:

$$\sum_{i=0}^p \epsilon^i Dx_i + \epsilon \left(\sum_{k_0+k_1+\dots+k_p=q} \frac{q!}{k_1!k_2!\dots k_p!} \epsilon^{\sum_{i=0}^p ik_i} \prod_{i=0}^p x_i^{k_i} \right) = f \quad (2)$$

54 The LHS of equation (3) is a polynomial of ϵ . Since it holds for all values of ϵ , the 0^{th} order term
55 of LHS should be equal to the RHS and the coefficients of all higher-order terms of ϵ should all be
56 0. Therefore, for the 0^{th} order, we obtain: $Dx_0 = f$, and more generally for the j^{th} order, where
57 $1 \leq j \leq p$, we have:

$$Dx_j = - \sum_{\substack{k_0+k_1+\dots+k_p=q \\ \sum_{i=0}^p ik_i=j-1}} \frac{q!}{k_1!k_2!\dots k_p!} \prod_{i=0}^p x_i^{k_i} := f_j \quad (3)$$

58 where f_j is the forcing function for j^{th} ODE. The first few terms for this expansion look like:

$$Dx_0 = f \quad Dx_1 = -x_0^2 \quad Dx_2 = -2x_0x_1 \quad \dots \quad (4)$$

59 The forcing function f_j depends only on previously solved x_i 's. Therefore, (1) is reduced to a series
60 of $p + 1$ linear ODEs of the same form: $Dx_j = f_j$ that can be solved iteratively. There are a variety
61 of ways to ensure that the initial boundary conditions are met. The main concept is to fix all $p + 1$
62 boundary conditions to be the same, so that the total solution's, x , boundary condition is satisfied;
63 that is, for all $k = 0, 1, \dots, p$, $x_k(t = 0) = x^* / \sum_{i=0}^p \epsilon^i$ and $\frac{d^j}{dt^j} x_k(t = 0) = x^{(j)*} / \sum_{i=0}^p \epsilon^i$.

64 Multi-head Fully Connected Neural Network

65 As established earlier, solving the non-linear ODE is equivalent to solving a sequence of linear
66 ODEs in the form $Dx = f$. To minimize computational complexity, we transform higher-order
67 differential equations into first-order equations by introducing $m - 1$ additional dependent variables
68 for an m^{th} order differential equation. Let $\mathbf{u} = [x, x^{(1)}, x^{(2)}, \dots, x^{(m-1)}]^T$ be a function mapping
69 from \mathbb{R} to \mathbb{R}^m , where $x^{(1)} = \dot{x}$ and $x^{(i)} = \dot{x}^{(i-1)}$ for $i = 2, \dots, m - 1$. The equation $Dx = f$ is
70 then reduced to a first-order linear ODE system (see Appendix C for details).

$$\begin{cases} \dot{x} - x^{(1)} = 0 \\ \dot{x}^{(i-1)} - x^{(i)} = 0, i = 2, 3, 4, \dots, m - 1 \\ g_0 x + \sum_{i=1}^{m-1} g_i x^{(i)} + g_m \dot{x}^{(m-1)} = f \end{cases} \quad (5)$$

71 Equation 5 is equivalent to: $B\dot{\mathbf{u}} + A\mathbf{u} = F_j$ with boundary conditions $\mathbf{u}(t=0) = \mathbf{u}^* \in \mathbb{R}^m$, where
 72 $\dot{\mathbf{u}} = [\dot{x}, \dot{x}^{(1)}, \dot{x}^{(2)}, \dots, \dot{x}^{(m-1)}]^T$ and $F_j = [0, 0, \dots, f_j]^T$. A detailed description of the matrices A
 73 and B can be found in Appendix A.

74 We create a fully connected neural network with K heads in two parts to approximate the K functions
 75 $\{\mathbf{u}_k\}_{k=1}^K$. The first part connects a 1D input to hidden layers, with the last layer having
 76 dimension mh . The activations of the last hidden layer are reshaped into a matrix $H \in \mathbb{R}^{m \times h}$,
 77 which reflects the hidden state of the ODE class and is then passed to the second part of the network.
 78 H connects to K heads, each associated with a linear ODE system. The output of each head is
 79 $\hat{\mathbf{u}}_k = HW_k \in \mathbb{R}^m$. A diagram of the general structure of the network can be found in Appendix B.
 80 The loss function for the k^{th} head in the network is defined over a sampled data set T as :

$$L_k = \frac{1}{mN} \sum_{t \in T} \|B_k \dot{\hat{\mathbf{u}}}_k(t) + A_k \hat{\mathbf{u}}_k(t) - F_k(t)\|_2^2 + \frac{1}{m} \|\hat{\mathbf{u}}_k(0) - \mathbf{u}_k^*\|_2^2 \quad (6)$$

81 where \mathbf{u}_k^* is the boundary condition of the k^{th} ODE. The total loss of the network is defined as:
 82 $L_{total} = \frac{1}{K} \sum_{k=1}^K L_k$ The purpose of training this neural network is to learn the latent space for
 83 one class of linear ODEs. Ideally, the larger K is, the better the learning of latent space and hence a
 84 generalization to a wider range of parameters.

85 One-Shot Transfer Learning

86 After training, we freeze the weights in the hidden layers. When encountering a new ODE of the
 87 same class, we only use one head, and the weights in this head can be calculated analytically in
 88 one shot. Suppose W is the time-independent network parameter in the last layer. The network
 89 now becomes: $\hat{\mathbf{u}}(t) = H(t)W$. We get the loss for this single-head neural network by substituting
 90 $\hat{\mathbf{u}}_k = \hat{\mathbf{u}}(t) = H(t)W$ into Eq. 6:

$$L = \frac{1}{mN} \sum_{t \in T} \|B\dot{H}_t W + AH_t W - F(t)\|_2^2 + \frac{1}{m} \|H_0 W - \mathbf{u}^*\|_2^2 \quad (7)$$

91 where H_t is the hidden state of the network evaluated at t and H_0 is the hidden state at the boundary.
 92 Differentiating L from W and setting $\frac{dL}{dW} = 0$, we obtain (details omitted):

$$W = M^{-1} \left(H_0^T \mathbf{u}^* + \frac{1}{N} \sum_{t \in T} B\dot{H}_t F(t) + \frac{1}{N} \sum_{t \in T} H_t^T A^T F(t) \right) \quad (8)$$

$$M = \frac{1}{N} \sum_{t \in T} (\dot{H}_t^T B^T B\dot{H}_t + \dot{H}_t^T B^T A H_t + H_t^T A^T B\dot{H}_t + H_t^T A^T A H_t) + H_0^T H_0 \quad (9)$$

93 For a fixed Duffing equation, the matrices A and B are fixed for all its $p+1$ reduced ODE systems.
 94 Thus, M only needs to be computed and inverted once. We only need to update the forcing function
 95 F in 8 which iteratively depends on previous solutions. By reusing the first part of the neural network
 96 and using only one head, we optimally and iteratively compute the head parameters for each ODE
 97 system to solve them.

98 3 Result

99 We applied our proposed methodology to the 1D Duffing equation. The Duffing equation we are inter-
 100 ested in 10 is a second order non-linear ODE with five parameters: $\delta, \alpha, \beta, \gamma, \omega$ and one boundary
 101 condition $x(0) = x^*$. All higher-order boundary conditions are set to 0.

$$\frac{d^2 x}{dt^2} + \delta \frac{dx}{dt} + \alpha x + \beta x^3 = \gamma \cos(\omega t) \quad (10)$$

102 Using our framework, we first utilized the perturbation method and introduced new variables to
 103 reduce the Duffing equation to a series of $p+1$ first-order linear ODE systems of the form: $\dot{u}_i +$

104 $Au_i = F_i$. We then built a network described in Section 2.2 with 10 heads. Each head represents a
 105 unique parameter setting. The specific details of the network structure can be found in Appendix B.
 106 The 10 parameter sets are uniformly randomly generated in the following range:

$$\gamma \in (0.5, 3), \omega \in (0.5, 3), \alpha \in (0.5, 4.5), \delta \in (0.5, 4.5), \mathbf{u}_1^* \in (-3, 3) \quad (11)$$

107 and $\mathbf{u}_2^* = 0$. After training (details in Appendix B), the network can accurately solve the 10 systems,
 108 and it acquires a significant understanding of the latent space of the not-linear ODE. We then test
 109 our method on an unseen Duffing equation. We measure the performance of the TL solution by
 110 computing the ODE loss of the Duffing equation. We used 14 different values of p to solve and
 111 approximate the solution. As shown in Figure 1(a), as the p value increases, the Duffing ODE loss
 112 decreases to around $10^{-3.75}$. The elbow shape can be used to figure out how many terms should be
 113 included in the perturbation expansion p .

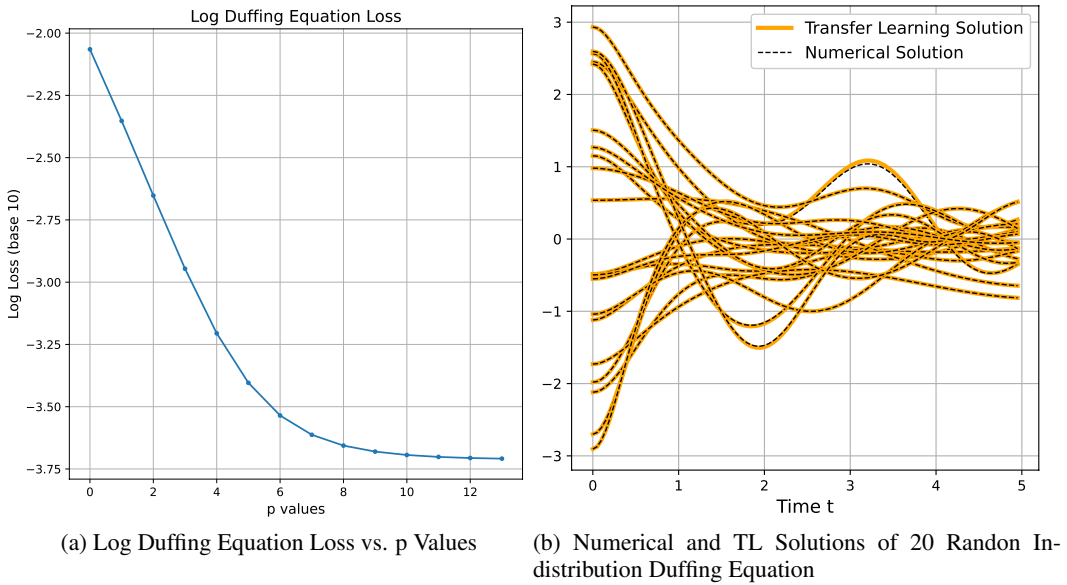


Figure 1

114 We also test our method by comparing the transfer learning solutions with numerical solutions (ex-
 115 plicit Runge-Kutta method of order 8) on 20 randomly generated Duffing equations in the same
 116 parameter range 11 (we fix $\beta = 0.5$ and $p = 12$). Each Duffing equation can be solved in seconds.
 117 (Details in Appendix B) As shown in Figure 2(b), the 20 transfer learning solutions align almost per-
 118 fectly with the numerical solutions, indicating that our methodology is very effective on equations
 119 in the same parameter range 11.

120 4 Conclusion

121 We introduced a framework using perturbation and one-shot transfer learning on PINNs to efficiently
 122 solve non-linear ODEs. We reduced non-linear ODEs to linear ODEs, trained a neural network with
 123 k heads to handle them, and derived a formula for network weights. This approach allows us to
 124 solve various non-linear ODEs of the same form with a single trained network. Future work aims to
 125 extend this methodology to various non-linear ODE and PDE systems.

126 Our work should be considered as a starting point for this methodology. Future work is needed to
 127 extend the framework to non-linear ODE and PDE systems with various non-linearity forms.

References

- 128
- 129 [1] CHANTADA, A. T., LANDAU, S. J., PROTOPAPAS, P., SCÓCCOLA, C. G., AND GARRAFFO,
130 C. Cosmology-informed neural networks to solve the background dynamics of the universe.
131 *Phys. Rev. D* 107 (Mar 2023), 063523.
- 132 [2] CHEN, FEIYU, E. A. Neurodiffee: A python package for solving differential equations with
133 neural networks. *Journal of Open Source Software* (2020).
- 134 [3] FESSER, L., QIU, R., AND D'AMICO-WONG, L. Understanding and mitigating extrapolation
135 failures in physics-informed neural networks, 2023.
- 136 [4] FLAMANT, C., PROTOPAPAS, P., AND SONDAK, D. Solving differential equations using
137 neural network solution bundles, 2020.
- 138 [5] GRAF, O., FLORES, P., PROTOPAPAS, P., AND PICHARA, K. Error-aware b-pinns: Improving
139 uncertainty quantification in bayesian physics-informed neural networks, 2022.
- 140 [6] HAO, Z., LIU, S., ZHANG, Y., YING, C., FENG, Y., SU, H., AND ZHU, J. Physics-informed
141 machine learning: A survey on problems, methods and applications, 2023.
- 142 [7] J. KEVORKIAN, J. D. C. *Perturbation Methods in Applied Mathematics*. Springer New York,
143 NY, 2010.
- 144 [8] KARNIADAKIS, G. E., KEVREKIDIS, I. G., LU, L., PERDIKARIS, P., WANG, S., AND
145 YANG, L. Physics-informed machine learning. *Nature Reviews Physics* (2021).
- 146 [9] KRISHNAPRIYAN, A., GHOLAMI, A., ZHE, S., KIRBY, R., AND MAHONEY, M. W. Char-
147 acterizing possible failure modes in physics-informed neural networks. In *Advances in Neural*
148 *Information Processing Systems* (2021), M. Ranzato, A. Beygelzimer, Y. Dauphin, P. Liang,
149 and J. W. Vaughan, Eds., vol. 34, Curran Associates, Inc., pp. 26548–26560.
- 150 [10] LAGARIS, I., LIKAS, A., AND FOTIADIS, D. Artificial neural networks for solving ordinary
151 and partial differential equations. *IEEE Transactions on Neural Networks* 9, 5 (1998), 987–
152 1000.
- 153 [11] LAWAL, Z. K., YASSIN, H., LAI, D. T. C., AND CHE IDRIS, A. Physics-informed neural
154 network (pinn) evolution and beyond: A systematic literature review and bibliometric analysis.
155 *Big Data and Cognitive Computing* 6, 4 (2022).
- 156 [12] LIU, S., HUANG, X., AND PROTOPAPAS, P. Residual-based error bound for physics-informed
157 neural networks, 2023.
- 158 [13] LU, LU, E. A. Deepxde: A deep learning library for solving differential equations. *CoRR*
159 (2019). <https://arxiv.org/abs/1907.04502>.
- 160 [14] MATTHEAKIS, M., PROTOPAPAS, P., SONDAK, D., GIOVANNI, M. D., AND KAXIRAS, E.
161 Physical symmetries embedded in neural networks, 2020.
- 162 [15] NASCIMENTO, R. G., FRICKE, K., AND VIANA, F. A. A tutorial on solving ordinary dif-
163 ferential equations using python and hybrid physics-informed neural network. *Engineering*
164 *Applications of Artificial Intelligence* 96 (2020), 103996.
- 165 [16] PELLEGRIN, R., BULLWINKEL, B., MATTHEAKIS, M., AND PROTOPAPAS, P. Transfer
166 learning with physics-informed neural networks for efficient simulation of branched flows.
167 *arXiv preprint arXiv:2211.00214* (2022).
- 168 [17] PROTOPAPAS, P., E. A. One-shot transfer learning of physics-informed neural networks. *CoRR*
169 (2021). <https://arxiv.org/abs/2110.11286>.
- 170 [18] ZOU, Z., AND KARNIADAKIS, G. E. L-hydra: Multi-head physics-informed neural networks,
171 2023.

Supplementary Material

172

Appendix A

173

174 The matrix B 12 is an m by m diagonal matrix in which the first $m-1$ diagonals are all 1 and the last
 175 diagonal is g_m . Matrix A 12 is an m by m matrix whose second upper diagonal entries are all -1 and
 176 last row is $[g_0, g_1, \dots, g_{m-1}]$.

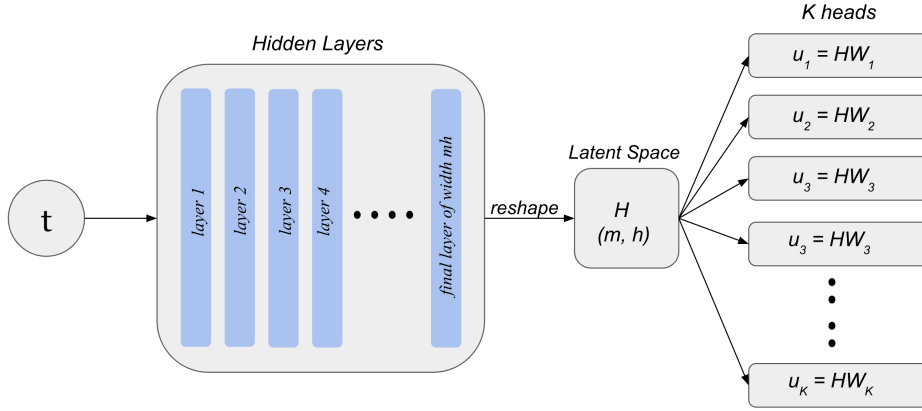
$$B = \begin{bmatrix} I_{m-1 \times m-1} & \vec{0} \\ \vec{0}^T & g_m \end{bmatrix}, A = \begin{bmatrix} 0 & -1 & 0 & \cdots & \cdots & 0 \\ 0 & 0 & -1 & \cdots & \cdots & 0 \\ 0 & 0 & 0 & -1 & \cdots & \vdots \\ \vdots & \vdots & \vdots & 0 & \ddots & 0 \\ 0 & 0 & 0 & \cdots & 0 & -1 \\ g_0 & g_1 & g_2 & \cdots & \cdots & g_{m-1} \end{bmatrix} \quad (12)$$

177

Appendix B

178 Here we show the diagram of the general multi-head PINN structure. In our real implementation
 179 to solve Duffing Equation, the network has 4 layers of hidden layers with width 256, 256, 256, 512
 180 respectively. Hidden layers are all connected by \tanh activation functions. The activations of the
 181 last hidden layer is reshaped into a matrix $H \in \mathbb{R}^{2 \times 256}$. The matrix H is connected to 10 heads of
 182 dimension 2 by a linear transform.

Figure 2: General Multihead PINN structure



183 To train the network, we used Adam optimizer for 5000 iterations with an initial learning rate of
 184 2×10^{-4} . Note that we applied an exponential decay to the learning rate: the learning rate is
 185 multiplied by a factor of 0.96 each 100 iterations. 200 random data points are uniformly generated
 186 in the domain $(0, 5)$ in each iteration as a sample set to compute the ODE loss. After 5000 iterations,
 187 the total loss (the sum of ODE loss and boundary loss) is reduced below 10^{-4} .

188 We ran our code on google colab using an Intel Xeon CPU with 2 vCPUs (virtual CPUs) and 51GB
 189 of RAM. Solving an unseen Duffing equations generally takes $0.5p + 1$ seconds, where $p + 1$ is the
 190 number of linear ODE systems we reduce to using perturbation method and the additional 1 s is the
 191 time to compute and invert the matrix M .

192

Appendix C

193 To reduce the ODE $Dx = f$ to first order, we introduce $m - 1$ time-dependent variables: $\{x^{(i)}\}_{i=1}^{m-1}$
 194 to form a function $\mathbf{u} : \mathbb{R} \rightarrow \mathbb{R}^m$. $\mathbf{u} = [x, x^{(1)}, x^{(2)}, \dots, x^{(m-1)}]^T$. $Dx = f$ is equivalent to:

$$g_0x + \sum_{i=1}^m g_i \frac{d^i}{dt^i} x = f \quad (13)$$

195 The introduced variables are defined as: $x^{(1)} = \dot{x}$ and $x^{(i)} = \dot{x}^{(i-1)}$ for $i = 2, 3, \dots, m - 1$. Expand
 196 these relations iteratively, we obtain $\frac{d^i}{dt^i} x = x^{(i)}$ for $i = 1, 2, \dots, m - 1$, plug into 13, we obtain:

$$g_0x + \sum_{i=1}^{m-1} g_i x^{(i)} + g_m \dot{x}^{(m-1)} = f \quad (14)$$

197 The definitions of these $m - 1$ variables introduces another $m - 1$ constraints, together with 14, we
 198 recover the linear ODE system in 5.